Dalton Transactions

PAPER

View Article Online
View Journal | View Issue

Cite this: *Dalton Trans.*, 2015, **44**, 747

Nickel complexes of a binucleating ligand derived from an SCS pincer†

Sonja M. Peterson, Monte L. Helm and Aaron M. Appel*

Received 5th September 2014,
Accepted 27th October 2014

DOI: 10.1039/c4dt02718c

www.rsc.org/dalton

A binucleating ligand has been prepared that contains an SCS pincer and three oxygen donor atoms in a partial crown ether loop. To enable metalation with Ni^0, a bromoarene precursor was used and resulted in the formation of a nickel–bromide complex in the SCS pincer portion of the ligand. Reaction of the nickel complex with a lithium salt yielded a heterobimetallic complex with bromide bridging the two metal centers. The solid-state structures were determined for this heterobimetallic complex and the nickel–bromide precursor, and the two complexes were characterized electrochemically to determine the influence of coordinating the second metal.

Introduction

The controlled positioning of two different metals with suitable proximity and orientation for small molecule activation remains a challenge.[1–26] The design of heterobimetallic complexes that incorporate a Lewis acid in close proximity to a redox tunable metal may be facilitated by using ligands containing very dissimilar donor atoms, such that the binding of the two different metals at the two different sites is selective. The ligand platform, H**L**, shown in Fig. 1 was originally developed by Vögtle for alkali metal ion complexation.[27,28] Later, Loeb improved the synthesis and studied palladium complexes with this ligand as metalloreceptors, demonstrating the selective binding of protic substrate molecules that also interacted with the oxygen atoms through hydrogen bonding.[29–32] In one report, after addition of excess silver triflate to the Pd(**L**)Cl complex, a Ag^+ ion was encapsulated forming a bimetallic complex.[33] To our knowledge, no other bimetallic complexes have been reported for this ligand or derivatives thereof.

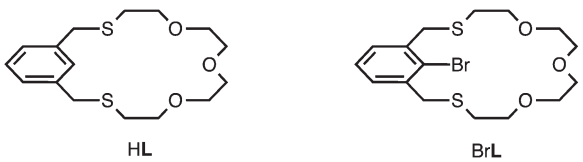

Fig. 1 Structures of HL and Br**L**.

Pacific Northwest National Laboratory, P.O. Box 999, MS K2-57, Richland, WA 99352, USA. E-mail: aaron.appel@pnnl.gov; Tel: +1-509-375-2157

†Electronic supplementary information (ESI) available: Crystallographic CIF files for the solid state structures and NMR spectra. CCDC 1023019 and 1023020. For ESI and crystallographic data in CIF or other electronic format see DOI: 10.1039/c4dt02718c

In this paper, we report the synthesis, structure, and electrochemical data for the nickel complexes of this macrocyclic, thiacyclophane ligand **L**, both with and without a lithium ion bound to the oxygen atoms.

Results

The ligand 17-bromo-5,8,11,-trioxa-2,14-dithia[15]-*m*-cyclophane (Br**L**) was prepared as an analog of H**L**.[31] This modification enabled metalation by nickel without the requisite C–H bond activation, which is more typical of the palladium analogs. The ligand was formed as a colorless oil in 54% yield from the slow addition of tetra(ethylene glycol) dithiol and 2-bromo-1,3-bis(bromomethyl)benzene to a suspension of Cs_2CO_3 in DMF at 60 °C (Scheme 1). The product, Br**L**, was characterized by ^{1}H NMR spectroscopy, and the spectrum contained four sets of resonances corresponding to the OCH_2, SCH_2, benzylic, and aromatic protons, analogous to H**L**.

The SCS-pincer Ni complex, Ni(**L**)Br, was prepared by oxidative addition of the ligand to $[Ni(cod)_2]$ at −78 °C.[34] The product was obtained as a diamagnetic orange crystalline solid in 41% yield. The complex was characterized by ^{1}H NMR spectroscopy, elemental analysis, and X-ray crystallography. In the ^{1}H NMR spectrum, the chemical shifts of Ni(**L**)Br compared to Br**L** were shifted upfield for the aromatic protons

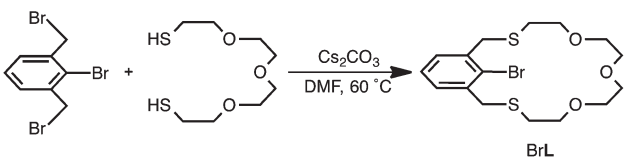

Scheme 1 Preparation of Br**L**.

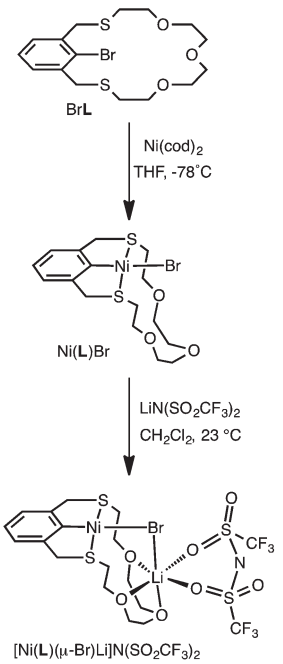

Scheme 2 Preparative route to Ni(L)Br and $[Ni(L)(\mu\text{-}Br)Li]N(SO_2CF_3)_2$ complexes.

($\Delta\delta$ = 0.47 ppm). The benzylic, OCH_2, and SCH_2 protons were no longer distinguishable and ranged from δ 4.66–2.80 ppm, but these resonances integrate to the total number of protons expected.

Treatment of Ni(**L**)Br with $LiN(SO_2CF_3)_2$ yielded $[Ni(L)(\mu\text{-}Br)Li]N(SO_2CF_3)_2$ as a dark orange crystalline solid in 94% yield (Scheme 2). The product was characterized by ^{1}H NMR spectroscopy, elemental analysis, and X-ray crystallography. Small changes in the ^{1}H NMR spectrum were observed when compared to Ni(**L**)Br, however, the benzylic, OCH_2, and SCH_2 protons were still not distinguishable.

Single crystals of Ni(**L**)Br and $[Ni(L)(\mu\text{-}Br)Li]N(SO_2CF_3)_2$ suitable for X-ray diffraction were obtained by layering solutions of the complexes in dichloromethane with hexanes. The molecular structure of Ni(**L**)Br is shown in Fig. 2, with selected bond lengths and angles in Table 1. The Ni^{II} center has a square planar geometry with three donor atoms provided by the SCS chelate, for which the bond distances are 2.1620(8) for Ni(1)–S(1), 2.1590(8) Å for Ni(1)–S(2), and 1.895(3) Å for Ni–C(1). All three of these bond distances are comparable to the only other structurally characterized nickel complex with a SCS chelating ligand (lacking the polyether chain), which was reported by Gebbink and van Koten.[34] The two five-membered chelate rings display bite-angles of 87.51(13)° and 87.89(13)° for S(1)–Ni(1)–C(1) and S(2)–Ni(1)–C(1), respectively, while the S(1)–Ni–S(2) angle shows a minor distortion from ideal, square planar geometry with an angle of 170.99(5)°. The fourth site *trans* to the Ni–C bond is occupied by a bromide ion with Ni–Br bond distance 2.3744(5) Å and a Br(1)–Ni(1)–C(1) angle of 179.16(14)°. The angles at the sulfur atoms: C(3)–S(1)–C(9) and C(8)–S(2)–C(16) are 102.5(2)° and 103.0(2)°. The coordination of the nickel to this ligand results in a structure in which the plane formed by the three oxygen atoms of the polyether loop is approximately orthogonal to the axis formed by the C–Ni–Br bonds.

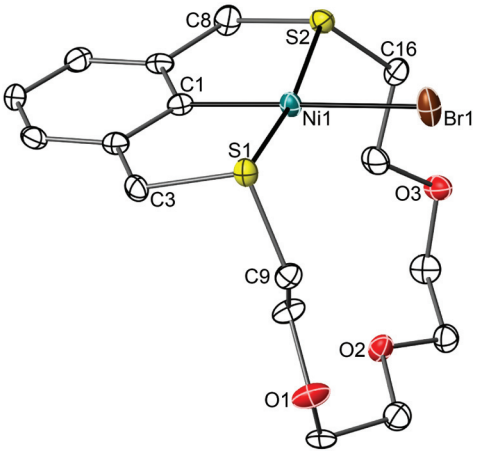

Fig. 2 Thermal ellipsoid diagram depicting the molecular structure of Ni(L)Br. Ellipsoids are drawn at 50% probability, and the hydrogen atoms are omitted for clarity.

Table 1 Selected bond distances (Å) and angles (°) for Ni(L)Br

Selected bond distances (Å) and angles (°) for Ni(L)Br	
Ni1–S1	2.1620(8)
Ni1–S2	2.1590(8)
Ni1–C1	1.895(3)
Ni1–Br1	2.3744(5)
S1–Ni1–C1	87.51(13)
S2–Ni1–C1	87.89(13)
S1–Ni1–S2	170.99(5)
Br1–Ni1–C1	179.16(14)
C3–S1–C9	102.5(2)
C8–S2–C16	103.0(2)

The molecular structure of $[Ni(L)(\mu\text{-}Br)Li]N(SO_2CF_3)_2$ contained the expected heterobimetallic complex shown in Fig. 3,

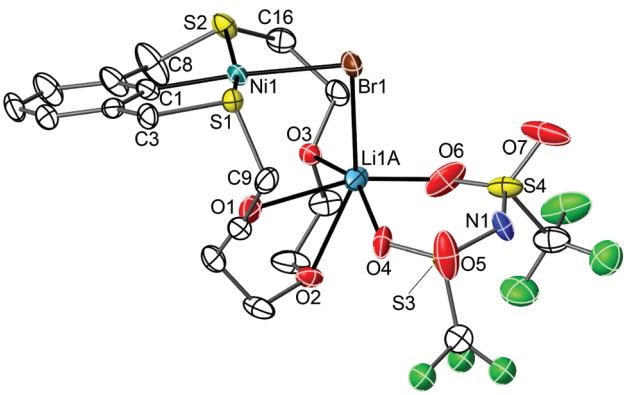

Fig. 3 Thermal ellipsoid plot depicting the molecular structure of $[Ni(L)(\mu\text{-}Br)Li]N(SO_2CF_3)_2$. One of the two disordered positions of the polyether ring and Li ion is shown. Ellipsoids are drawn at 50% probability, and the hydrogen atoms are omitted for clarity.

Table 2 Selected bond distances (Å) and angles (°) for [Ni(L)(μ-Br)Li]-$N(SO_2CF_3)_2$

Ni1–S1	2.1665(8)
Ni1–S2	2.1645(9)
Ni1–C1	1.901(3)
Ni1–Br1	2.3969(5)
Li1A–Br1	2.99(2)
Li1–Br1	2.71(2)
S1–Ni1–C1	87.55(9)
S2–Ni1–C1	85.03(9)
S1–Ni1–S2	163.40(4)
Br1–Ni1–C1	175.78(9)
C3–S1–C9	102.00(15)
C8–S2–C16	102.53(18)
Ni1–Br1–Li1A	78.2(4)
Ni1–Br1–Li1	85.8(4)

with select bond lengths and angles shown in Table 2. The Ni^{II} center retains the same SCS primary coordination sphere with square planar geometry and comparable bond lengths to the Ni(**L**)Br complex, with bond distances of 2.1665(8) Å for Ni1–S1, 2.1645(9) Å for Ni1–S2, and 1.901(3) Å for Ni–C1. The two five-membered chelate rings display bite-angles of 87.55 (9)° for S(1)–Ni(1)–C(1) and 85.03(9)° for S(2)–Ni(1)–C(1), while the S(1)–Ni(1)–S(2) angle is 163.40(4)°, thereby showing a distortion from ideal, square planar geometry. The fourth site *trans* to the Ni–C bond is still occupied by a bromide ion with Ni–Br bond distance 2.3969(5) Å and a Br(1)–Ni(1)–C(1) angle of 175.78(9)°. The slight lengthening of the Ni–Br bond distance is expected since the bromide ion is bridged between the nickel and lithium ions, although this Ni–Br bond is shorter than the only other reported example of a Ni–Br–Li bridge which has a Ni–Br bond length of ~2.45 Å.[35] In the structure of [Ni(**L**)(μ-Br)Li]$N(SO_2CF_3)_2$, the angles at the sulfur atoms are 102.00(15)° for C(3)–S(1)–C(9) and 102.53(18)° for C(8)–S(2)–C(16), which again results in the orientation of the three oxygen atoms of the polyether loop to be approximately orthogonal to the axis formed by the C–Ni–Br bonds. The oxygen atoms of the polyether chain act to stabilize and partially encapsulate the Li ion in a distorted octahedral geometry, in which the three oxygens from the polyether chain are coordinated facially. Due to the apparent flexibility of the polyether ring, the crystal structure was disordered with two different positions for the Li ion and the polyether ring. The counter ion, bis(trifyl)imide, is also coordinated to the Li ion through two of the oxygen atoms forming a bidentate chelating ring. This coordination mode has been reported for several complexes containing $LiN(SO_2CF_3)_2$.[36–39] The final ligand is the bromide ion that bridges to the Ni^{II} ion. The Li–Br(1) distance is 2.71(2) for Li(1)–Br(1) and 2.99(2) Å for Li(1A)–Br(1). Both bonds are longer than typical reported Li–Br bonds in M–Br–Li bridges (~2.52 Å),[35,40,41] and are approximately at the sum of the ionic radii for lithium and bromide. The Ni–Br–Li angles are 85.8(4)° for Ni(1)–Br(1)–Li(1) and 78.2(4)° for Ni(1)–Br(1)–Li(1A). The average Ni–Li bond distance for either structure is 3.46 Å, indicating that a metal-metal interaction is unlikely, given that this distance is essentially equivalent to the sum of the van der Waals radii for the two elements.

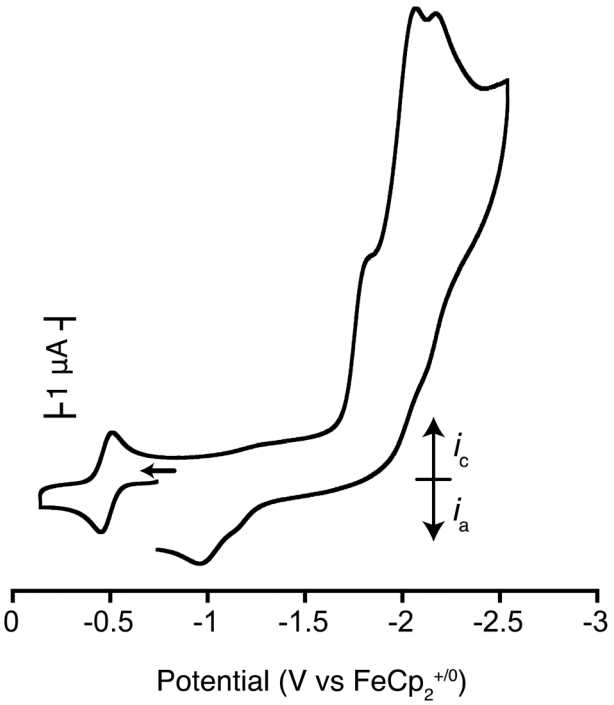

Fig. 4 Cyclic voltammogram of 0.5 mM Ni(L)Br, with $FeCp^*_2$ used as an internal reference (at −0.5 V *vs.* $FeCp_2^{+/0}$). Conditions: 0.2 M Et_4NBF_4 in CH_3CN; 1 mm glassy carbon working electrode; scan rate 0.5 V s^{-1} at 25 °C.

Electrochemical studies

Study of Ni(**L**)Br by cyclic voltammetry resulted in the voltammogram shown in Fig. 4. Three irreversible reduction waves are observed with peak potentials of −1.81, −2.05, and −2.16 V *vs.* the $FeCp_2^{+/0}$ couple in acetonitrile at a scan rate of 0.5 V s^{-1}. These reduction peaks were chemically irreversible at all observed scan rates (up to 5 V s^{-1}). Similarly, the cyclic voltammogram of [Ni(**L**)(μ-Br)Li]$N(SO_2CF_3)_2$ is shown in Fig. 5, and this complex has analogous electrochemical behavior to that for Ni(**L**)Br. Two irreversible reduction waves are observed peak potentials of −2.03 and −2.35 V *vs.* the $FeCp_2^{+/0}$ couple in acetonitrile at a scan rate of 0.5 V s^{-1}, and these peaks remain chemically irreversible at all observed scan rates (up to 5 V s^{-1}).

Discussion

A variation of a SCS pincer-ligand and the corresponding nickel complex have been synthesized and characterized. While analogous to the previously reported palladium complex,[31,33] the use of a bromoarene starting material was necessary due to the inability of nickel to perform the required C–H bond activation to achieve the tridentate coordination mode illustrated in Scheme 2. Starting from the newly synthesized bromoarene, Br**L**, and $Ni(cod)_2$, the installation of nickel was successful to yield the neutral nickel(II) complex, Ni(**L**)Br.

The use of $\mathbf{L}^-$ as a binucleating ligand has not been previously reported, with the exception of a palladium and silver

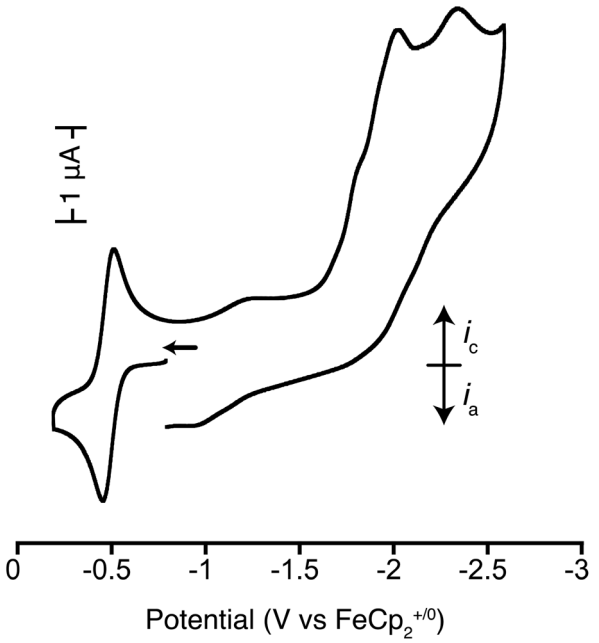

Fig. 5 Cyclic voltammogram of 1.5 mM [Ni(**L**)(μ-Br)Li]N$(SO_2CF_3)_2$, with $FeCp^*_2$ used as an internal reference (at −0.5 V *vs.* $FeCp_2^{+/0}$). Conditions: 0.2 M Et_4NBF_4 in CH_3CN; 1 mm glassy carbon working electrode; scan rate 0.5 V s^{-1} at 25 °C.

complex that resulted from attempted halide abstraction from Pd(**L**)Cl.[33] By reacting Ni(**L**)Br with LiN$(SO_2CF_3)_2$, a heterobimetallic complex was prepared. The solid-state structure of this complex, [Ni(**L**)(μ-Br)Li]N$(SO_2CF_3)_2$, has a bridging bromide between the two metal ions and additionally contains a second anion that is coordinated to the complex, as shown in Scheme 2 and Fig. 3. In contrast to the bridging bromide, this second anion, $^-N(SO_2CF_3)_2$, has no direct association with nickel, but rather is a bidentate ligand for lithium, resulting in a distorted octahedral coordination environment for this cation. The binding of the $^-N(SO_2CF_3)_2$ anion to the lithium suggests that the partial-crown ether loop and bromide are insufficient to coordinatively saturate lithium. While the two metals are in relatively close proximity, the distance between them (3.46 Å) is large enough that no M–M bonding is expected, as this distance is equivalent to the sum of the van der Waals radii for the two elements.

Electrochemical studies of Ni(**L**)Br and [Ni(**L**)(μ-Br)Li]N-$(SO_2CF_3)_2$ by cyclic voltammetry show chemically irreversible reductions, consistent with previous studies of related complexes, such as PCP pincer-complexes of nickel.[42,43] Additionally, the negative potentials observed for the two reduction waves of each complex are in line with previous studies of anionic carbene pincer ligands with group 10 metals.[44,45] The addition of LiN$(SO_2CF_3)_2$ to the nickel complex did not have a large effect on the potentials or general features observed in the cyclic voltammetry studies, suggesting that the coordination of the lithium cation to bromide had little effect on the electronic properties of the nickel center. This observation is consistent with the very limited change in Ni–Br distance between the structures with and without lithium, but does not preclude a significant difference in stabilization of the bridged species (in this case, bromide).

As illustrated in Fig. 3 and Scheme 2, the use of $\mathbf{L}^-$ to position two distinct metals in close proximity provides an opportunity to synthesize structures reminiscent of the active site of [NiFe] CO-dehydrogenase. The use of nickel as a reducible and potentially nucleophilic metal, in combination with lithium as an electrophilic metal, may enable reactivity towards CO_2 through stabilization of a bridging Ni–C(O)–O–Li structure. Investigations of [Ni(**L**)(μ-Br)Li]N$(SO_2CF_3)_2$ and related complexes for the reduction of CO_2 are underway in our laboratories.

Summary and conclusions

A ligand platform with distinct coordination sites was used to prepare a heterobimetallic complex containing an electroactive metal and an electrophilic metal. Substitution with bromide enabled preparation of a nickel complex of an SCS ligand containing an available partial crown-ether loop. The resulting nickel–bromide complex was reacted with a lithium salt to yield a heterobimetallic complex with a bridging bromide ligand. Solid-state structures were determined for both the starting nickel–bromide complex and the subsequent heterobimetallic complex. Electrochemical studies of both complexes indicated that the reduction events were complex, but not substantially affected by the addition of the second metal ion.

Experimental

General procedures

All synthetic procedures were performed under an atmosphere of N_2 using standard Schlenk or glovebox techniques. Unless described otherwise, all reagents were purchased from commercial sources (Strem and or Sigma-Aldrich) and were used as received. Solvents were dried by passage through activated alumina in an Innovative Technology, Inc., PureSolv solvent purification system. Deuterated chloroform was dried over CaH_2 and vacuum transferred before use. NMR spectra were recorded in thin walled NMR tubes (25 °C) on a Varian Inova 500 MHz spectrometer. ^1H chemical shifts were referenced to residual proton resonances in deuterated chloroform. Elemental analyses were performed by Atlantic Microlabs, Norcross, GA, with V_2O_5 as a combustion catalyst.

Preparation of BrL

The ligand Br**L** was prepared using a procedure analogous to that for H**L**.[34] To a suspension of Cs_2CO_3 (0.890 g, 2.72 mmol) in DMF (50 mL), at 60 °C, was added a solution of 2-bromo-1,3-bis(bromomethyl)benzene (0.454 g, 1.33 mmol) and tetra (ethylene glycol) dithiol (0.270 mL, 1.33 mmol) in DMF (50 mL) over 22.5 h. After the slow addition was complete, the DMF was removed by vacuum, leaving a tan oil and cesium

salts. The residue was dissolved in CH_2Cl_2 (100 mL), filtered, and the filtrate washing with 0.1 M NaOH (2 × 50 mL) and deionized water (50 mL) and then dried over anhydrous $MgSO_4$/activated carbon for 1 h. The solution was filtered and the CH_2Cl_2 evaporated to dryness *in vacuo*. The oil obtained after concentration of the filtrate was purified by flash chromatography over silica gel, eluting with 1 : 1 petroleum ether–diethyl ether. Colorless oil was obtained upon evaporation of the solvent. Yield: 0.290 g (54%). ^{1}H NMR ($CDCl_3$): δ (ppm) 7.40 (d, 2H, aromatic, J = 7.6 MHz), 7.28 (t, 1H, aromatic, J = 7.2 MHz), 4.00 (s, 4H, benzylic), 3.56–3.48 (m, 12H, OCH_2), 2.63 (t, 4H, SCH_2, J = 7.1 MHz). ^{13}C{^{1}H} NMR ($CDCl_3$): δ (ppm) 138.99, 129.61, 127.29, 126.93 (aromatic), 70.86, 70.59, 70.35 (CH_2O) 36.92 (benzylic), 30.28 (SCH_2). Anal. Calcd for $C_{16}H_{23}BrO_3S_2$: C, 47.17; H, 5.69. Found: C, 48.02; H, 5.98. The higher than expected carbon and hydrogen results are consistent with incomplete solvent removal due to the high viscosity of the resulting oil.

Preparation of Ni(L)Br

A yellow solution of [Ni(cod)$_2$] (0.068 g, 0.25 mmol) in THF (15 mL) was cooled to −78 °C and a solution of Br**L** (0.100 g, 0.245 mmol) in THF (5 mL) was added dropwise. The reaction was stirred for 30 min at −78 °C and subsequently allowed to warm to room temperature while stirring for 3 h. The solution remained yellow. The solvent was removed by vacuum, the resulting solid was dissolved in acetonitrile, and this solution was filtered. The solvent from the filtrate was removed by vacuum. The product was redissolved in dichloromethane and precipitated by adding hexanes. An orange solid was obtained after removal of all volatiles by vacuum. Orange crystals suitable for X-ray diffraction were obtained by layering a solution of the product in dichloromethane with hexanes. Crystalline yield: 0.047 g (41%). ^{1}H NMR ($CDCl_3$): δ (ppm) 6.95 (t, 1H, aromatic, J = 6.9 Hz), 6.79 (d, 2H, aromatic, J = 6.9 Hz), 4.69–2.79 (m, 20H, –CH_2). Anal. Calcd for $C_{16}H_{23}BrNiO_3S_2$: C, 41.23; H, 4.97. Found: C, 41.30; H, 5.08.

Preparation of [Ni(L)(μ-Br)Li]N(SO$_2$CF$_3$)$_2$

A yellow solution of Ni(**L**)Br (0.011 g, 0.024 mmol) in dichloromethane (1.5 mL) was stirred and Li[N(SO$_2$CF$_3$)$_2$] (0.007 g, 0.02 mmol) was added. The reaction was stirred for 1 h. The color of the solution darkened to orange. Orange crystals suitable for X-ray diffraction were obtained by layering a solution of the product in dichloromethane with hexanes. Crystalline yield: 0.017 g (94%). ^{1}H NMR ($CDCl_3$): δ (ppm) 6.97 (t, 1H, aromatic, J = 6.9 MHz), 6.8 (d, 2H, aromatic, J = 6.6 MHz), 4.46–2.81 (m, 20H, –CH_2). ^{19}F NMR ($CDCl_3$): δ = −79.08 (N(SO$_2$CF$_3$)$_2^-$). Anal. Calcd for $C_{18}H_{23}BrF_6LiNNiO_7S_4$: C, 28.70; H, 3.08; N, 1.86. Found: C, 28.50; H, 3.14; N, 1.94.

Electrochemistry

Cyclic voltammetry was performed on solutions of 0.2 mM complexes in 0.2 M of tetraethylammonium tetrafluoroborate (Et_4NBF_4) electrolyte in acetonitrile. Voltammograms with scan rates from 0.05 V s^{-1} to 5 V s^{-1} were taken under N_2. Cyclic voltammetry experiments were performed using a CH Instruments model 600D potentiostat. Measurements were performed using standard three-electrode cell containing a 1 mm glass carbon disc encased in PEEK glassy carbon working electrode, a 3 mm glassy carbon rod (Alfa) as the counter electrode, and a pseudo-reference electrode consisting of a silver wire suspended in electrolyte solution (0.2 M Et_4NBF_4 in MeCN) and separated from the analyte solution by a Vycor frit. Prior to the acquisition of each voltammogram, the working electrode was polished using 0.25 micron MetaDi diamond polishing paste (Buehler) and rinsed with deionized water. All potentials are reported *versus* the ferrocenium/ferrocene couple at 0.0 V using decamethylferrocene as an internal reference (at −0.50 V *vs.* $FeCp_2^{+/0}$ in MeCN).

X-ray diffraction studies

X-ray diffraction data was collected on a Bruker-AXS Kappa APEX II CCD diffractometer with 0.71073 Å Mo-Kα radiation. Selected crystals were mounted using NVH immersion oil onto a nylon fiber and cooled to the data collection temperature of 100–120 K. Unit cell parameters were obtained from 90 data frames, 0.3° Φ, from three different sections of the Ewald sphere. All structures were solved by direct methods using SHELXS-97 and refined with full-matrix least-squares procedures using SHELXL-97.[46] All non-hydrogen atoms are anisotropically refined unless otherwise reported; the hydrogen atoms were included in calculated positions as riding models in the refinement. Crystallographic data collection and refinement information can be found in the supporting material.

Acknowledgements

The research by SMP and AMA was supported by the US Department of Energy, Office of Science, Office of Basic Energy Sciences, Division of Chemical Sciences, Geosciences & Biosciences. The research by MLH was supported as part of the Center for Molecular Electrocatalysis, an Energy Frontier Research Center funded by the U.S. Department of Energy, Office of Science. Pacific Northwest National Laboratory (PNNL) is a multiprogram national laboratory operated for DOE by Battelle.

Notes and references

1 J.-H. Jeoung and H. Dobbek, *Science*, 2007, **318**, 1461–1464.
2 G. Bender, E. Pierce, J. A. Hill, J. E. Darty and S. W. Ragsdale, *Metallomics*, 2011, **3**, 797.
3 G. Fachinetti, C. Floriani and P. F. Zanazzi, *J. Am. Chem. Soc.*, 1978, **100**, 7405–7407.
4 S. Gambarotta, F. Arena, C. Floriani and P. F. Zanazzi, *J. Am. Chem. Soc.*, 1982, **104**, 5082–5092.
5 E. E. Benson, K. A. Grice, J. M. Smieja and C. P. Kubiak, *Polyhedron*, 2013, **58**, 229–234.

6 E. E. Benson, M. D. Sampson, K. A. Grice, J. M. Smieja, J. D. Froehlich, D. Friebel, J. A. Keith, E. A. Carter, A. Nilsson and C. P. Kubiak, *Angew. Chem., Int. Ed.*, 2013, **52**, 4841–4844.
7 J.-M. Savéant, *Chem. Rev.*, 2008, **108**, 2348–2378.
8 C. Costentin, S. Drouet, M. Robert and J.-M. Savéant, *Science*, 2012, **338**, 90–94.
9 D. Huang and R. H. Holm, *J. Am. Chem. Soc.*, 2010, **132**, 4693–4701.
10 X. Zhang, D. Huang, Y.-S. Chen and R. H. Holm, *Inorg. Chem.*, 2012, **51**, 11017–11029.
11 C. Uyeda and J. C. Peters, *Chem. Sci.*, 2013, **4**, 157–163.
12 C. Uyeda and J. C. Peters, *J. Am. Chem. Soc.*, 2013, **135**, 12023–12031.
13 J. P. Krogman, B. M. Foxman and C. M. Thomas, *J. Am. Chem. Soc.*, 2011, **133**, 14582–14585.
14 R. Dobrovetsky and D. W. Stephan, *Angew. Chem., Int. Ed.*, 2013, **52**, 2516–2519.
15 M. Rakowski DuBois and D. L. DuBois, *Acc. Chem. Res.*, 2009, **42**, 1974–1982.
16 M. Hammouche, D. Lexa, M. Momenteau and J.-M. Savéant, *J. Am. Chem. Soc.*, 1991, **113**, 8455–8466.
17 J. Agarwal, E. Fujita, H. F. Schaefer and J. T. Muckerman, *J. Am. Chem. Soc.*, 2012, **134**, 5180–5186.
18 Y. Hayashi, S. Kita, B. S. Brunschwig and E. Fujita, *J. Am. Chem. Soc.*, 2003, **125**, 11976–11987.
19 A. M. Appel, J. E. Bercaw, A. B. Bocarsly, H. Dobbek, D. L. DuBois, M. Dupuis, J. G. Ferry, E. Fujita, R. Hille, P. J. A. Kenis, C. A. Kerfeld, R. H. Morris, C. H. F. Peden, A. R. Portis, S. W. Ragsdale, T. B. Rauchfuss, J. N. H. Reek, L. C. Seefeldt, R. K. Thauer and G. L. Waldrop, *Chem. Rev.*, 2013, **113**, 6621–6658.
20 E. E. Benson, C. P. Kubiak, A. J. Sathrum and J. M. Smieja, *Chem. Soc. Rev.*, 2009, **38**, 89–99.
21 C. Finn, S. Schnittger, L. J. Yellowlees and J. B. Love, *Chem. Commun.*, 2012, **48**, 1392–1399.
22 J. R. Pinkes, B. D. Steffey, J. C. Vites and A. R. Cutler, *Organometallics*, 1994, **13**, 21–23.
23 T. A. Hanna, A. M. Baranger and R. G. Bergman, *J. Am. Chem. Soc.*, 1995, **117**, 11363–11364.
24 A. J. M. Miller, J. A. Labinger and J. E. Bercaw, *Organometallics*, 2011, **30**, 4308–4314.
25 M. J. Sgro and D. W. Stephan, *Angew. Chem., Int. Ed.*, 2012, **51**, 11343–11345.
26 S. J. Mitton and L. Turculet, *Chem. – Eur. J.*, 2012, **18**, 15258–15262.
27 F. Vögtle and E. Weber, *Angew. Chem., Int. Ed. Engl.*, 1974, **86**, 126–127.
28 E. Weber and F. Vögtle, *Eur. J. Inorg. Chem.*, 1976, **109**, 1803–1831.
29 J. E. Kickham and S. J. Loeb, *J. Chem. Soc., Chem. Commun.*, 1993, 1848–1850.
30 J. E. Kickham, S. J. Loeb and S. L. Murphy, *J. Am. Chem. Soc.*, 1993, **115**, 7031–7032.
31 J. E. Kickham and S. J. Loeb, *Inorg. Chem.*, 1994, **33**, 4351–4359.
32 J. E. Kickham and S. J. Loeb, *Inorg. Chem.*, 1995, **34**, 5656–5665.
33 J. E. Kickham and S. J. Loeb, *Organometallics*, 1995, **14**, 3584–3587.
34 C. A. Kruithof, H. P. Dijkstra, M. Lutz, A. L. Spek, R. J. M. K. Gebbink and G. van Koten, *Organometallics*, 2008, **27**, 4928–4937.
35 J. D. Masuda, P. Wei and D. W. Stephan, *Dalton Trans.*, 2003, 3500–3505.
36 M. Schmeisser, F. W. Heinemann, P. Illner, R. Puchta, A. Zahl and R. van Eldik, *Inorg. Chem.*, 2011, **50**, 6685–6695.
37 D. M. Seo, P. D. Boyle and W. A. Henderson, *Acta Crystallogr., E: Struct. Rep. Online*, 2011, **67**, m534–m534.
38 K. Matsumoto, R. Hagiwara and O. Tamada, *Solid State Sci.*, 2006, **8**, 1103–1107.
39 M. G. Davidson, P. R. Raithby, A. L. Johnson and P. D. Bolton, *Eur. J. Inorg. Chem.*, 2003, **2003**, 3445–3452.
40 J. Powell, A. Lough and F. Wang, *Organometallics*, 1992, **11**, 2289–2295.
41 V. Lorenz, S. Blaurock and F. T. Edelmann, *Z. Anorg. Allg. Chem.*, 2008, **634**, 2819–2824.
42 A. Castonguay, A. L. Beauchamp and D. Zargarian, *Organometallics*, 2008, **27**, 5723–5732.
43 A. Castonguay, D. M. Spasyuk, N. Madern, A. L. Beauchamp and D. Zargarian, *Organometallics*, 2009, **28**, 2134–2141.
44 B. D. Steffey, A. Miedaner, M. L. Maciejewski-Farmer, P. R. Bernatis, A. M. Herring, V. S. Allured, V. Carperos and D. L. DuBois, *Organometallics*, 1994, **13**, 4844–4855.
45 O. R. Luca, J. D. Blakemore, S. J. Konezny, J. M. Praetorius, T. J. Schmeier, G. B. Hunsinger, V. S. Batista, G. W. Brudvig, N. Hazari and R. H. Crabtree, *Inorg. Chem.*, 2012, **51**, 8704–8709.
46 G. M. Sheldrick, *Acta Crystallogr., Sect. A: Fundam. Crystallogr.*, 2008, **64**, 112–122.